Desalination and Water Treatment
www.deswater.com

doi: 10.1080/19443994.2015.1131635

57 (2016) 22454–22466
October

Taylor & Francis
Taylor & Francis Group

Adsorption of copper (Cu^{2+}) from aqueous solution using date palm trunk fibre: isotherms and kinetics

M.T. Amin*, A.A. Alazba, M. Shafiq

Alamoudi Water Research Chair, King Saud University, P.O. Box 2460, Riyadh 11451, Kingdom of Saudi Arabia, Tel. +96 6114673737; emails: mtamin@ksu.edu.sa (M.T. Amin), alazba@ksu.edu.sa (A.A. Alazba), msrana.c@ksu.edu.sa (M. Shafiq)

Received 20 August 2015; Accepted 6 December 2015

ABSTRACT

In this work, date palm trunk (DPT) fibre was investigated for the eviction of copper ions (Cu^{2+}) from aqueous solution. The surface chemistry of the DPT adsorbent was characterized through Fourier transform infrared spectroscopy and X-ray powder diffraction. The specific surface area and the average crystalline size of the DPT fibre adsorbent were measured as 2.104 $m^2\ g^{-1}$ and 320 nm, respectively. Equilibrium adsorption was achieved at 150 min and results reflected significantly higher adsorption of Cu^{2+} onto DPT fibre at pH 5 (6 mg g^{-1}, 12%) than at pH 2–4 (1–4 mg g^{-1}, 1–7%). The adsorption data revealed maximum removal (25.4 mg g^{-1}) at the adsorbent dose of 5 g L^{-1}. Significantly, removal (34 mg g^{-1}) was observed with particles 75 μm and Cu^{2+} removal was significantly higher (6–23 mg g^{-1}) with increasing Cu^{2+} concentration from 20 to 100 mg L^{-1}. Adsorption kinetics data were modelled using pseudo-first-order and pseudo-second-order kinetics. The behaviour and the nature of Cu^{2+} adsorption were analysed by employing the Langmuir, Freundlich, Harkins–Jura (H–J) and Dubinin–Radushkevich (D–R) isotherm models. The results reflect that the adsorption isotherm model fitted the experimental data in the following order: Langmuir (R^2, 0.9933) > H–J (R^2, 0.9869) > Freundlich (R^2, 0.9768) > D–R (R^2, 0.8827) with monolayer Cu^{2+} adsorption. The experimental data were best explained by a Langmuir isotherm model and pseudo-second-order kinetics with R^2 = 0.9933 and 0.9905, respectively, and q_{max} of 25.25 mg g^{-1} with chemisorption (E = 14.59 kJ mol^{-1}). The homogeneity of the adsorbent surface functional groups makes DPT suited for sequestering toxic Cu^{2+} from wastewater. Suitable physical, chemical and physicochemical surface modifications can further improve the adsorption capabilities of DPT adsorbents.

Keywords: Adsorption; Copper; DPT fibre; Kinetics; Isotherm models

1. Introduction

Heavy metal concentrations are increasing day by day with rapidly growing industry and urbanization [1]. Freshwater reserves are becoming unfit for use due to untreated waste disposal. Heavy metals are toxic even at low concentrations. They are non-biodegradable, and they tend to accumulate in living organisms and ultimately cause various diseases and disorders [2]. Heavy metals, such as lead (Pb^{2+}), copper (Cu^{2+}), cadmium (Cd^{2+}), zinc (Zn^{2+}), arsenic (As) (III–VI), nickel (Ni^{2+}), mercury (Hg^{2+}), manganese (Mn^{2+}) and chromium (Cr^{2+}), are important pollutants

*Corresponding author.

1944-3994/1944-3986 © 2016 Balaban Desalination Publications. All rights reserved.

of wastewater that are released by industries, from agriculture and by households.

Cu^{2+} releases from industries including mining, smelting, as well as industries that produce products from copper such as wire and pipes. Currently, the United States Environmental Protection Agency (EPA) has set its permissible limits as 1.3 mg L^{-1} in industrial effluents. The World Health Organization (WHO) defines a Cu^{2+} permissible limit of 1.5 mg L^{-1} in drinking water [3]. Exposure to copper may cause health problems such as kidney damage, miscarriages, disorders of the nervous system, subsequent vomiting, headache, nausea, respiratory problems, abdominal pain, liver and gastrointestinal bleeding and brain damage [4]. Therefore, the treatment of heavy metals from the effluent streams of various industries is necessary [5].

Several conventional methods, including chemical precipitation, lime softening [6], evaporation, membrane filtration, desalination, chemical coagulation and flocculation, ion exchange, electrodialysis and reverse osmosis [7–10], have been employed for heavy metal removal from industrial wastewaters. However, these methods have some limitations, which include high energy cost, production of oxidation by-products, need to regenerate ion exchange resins, bulk generation of toxic sludge in flocculation/coagulation methods, short ozone half-life in ozonation and membrane fouling during the filtration process. Moreover, these methods are also ineffective in case of high heavy metal concentrations (100 mg L^{-1}) in an aqueous solution [11].

On the other hand, adsorption has gained attraction in the industrial wastewater treatment compared to other techniques. Bulk availability of bioadsorbents, metal selectivity, simple design and easy operation, automation, capability of operation at very low concentration, lower initial costs and excellent resistance to the degenerative action of target contaminants are some advantages that make adsorption an attractive alternative for metal treatment [12–14]. The exhausted adsorbents can be regenerated with simple acid/alkali-based treatments [15]. Many adsorbents, such as *Sargassum acinarum* [16], grape seeds [17], lentil, wheat and rice shells [18], coconut tree sawdust, eggshell ES and sugarcane bagasse [19], oyster shell powder [20], black liquor [21] and mushroom biomass [22], have been investigated for copper removal from industrial wastewater.

Date palm is an important plant in hot and dry regions of Africa, the Middle East and Asia. The date palm fruit is well known as a staple food of these regions. Date production generates a huge amount of waste and by-products, e.g. date stones and date palm trunk (DPT) fibres. Therefore, there is great opportunity in these regions to use these abundantly available by-products as adsorbents for wastewater treatment. Many researchers have tried to use activated carbon from date stones as an adsorbent for heavy metal removal.

The goal of the present work was to explore the potential of DPT fibre for Cu^{2+} removal. The removal conditions and the best adsorption isotherms and kinetic models with their related constants were determined. The effect of contact time, pH, adsorbent dose and initial adsorbate concentrations on the adsorption capacity of DPT fibre are investigated.

2. Materials and methods

2.1. Chemicals and reagents

A stock solution of Cu^{2+} (1,000 mg L^{-1}) was prepared in deionized water by dissolving 3.917 g of copper sulphate pentahydrate ($CuSO_4{\cdot}5H_2O$; AR grade, Merck) salt in a 1,000 mL volumetric flask. Cu^{2+} working standard solutions in the range of 5−100 mg L^{-1} were prepared for use in the experiments by dilution of the 1,000 mg L^{-1} stock solution. Solution pH was adjusted using 0.1 M HCl and 0.1 M NaOH. pH measurements were carried out with a microprocessor-based pH metre (PHS-3CW; Bante Instruments, China).

2.2. Adsorbent preparation

A piece of dry DPT was collected from a local farm in Riyadh (Saudi Arabia). The date palm fibres were weaved and pulled out of the trunk in the form of a nearly rectangular mesh formed by layers superposed by the tree. The layers were easily separated when immersed in water, yielding individual fibres of diameter 0.2–0.8 mm, with an average size of approximately 0.5 mm. The DPT fibres were then washed three times with tap water with a good rubbing to remove all foreign particles, filtered out and soaked in distilled water for 30 min and filtered out again. The DPT fibres were then placed in drying oven at 105°C for 24 h. Afterwards, DPT fibres were crushed by a crushing machine. The powder was sieved using available sieves of nominal sizes (75, 150, and 250 μm). Particle sizes of 75 μm were used in all experiments throughout this work; the other sizes 150 and 250 μm were used only to examine the particle size effect in the batch study. DPT fibres were stored in airtight containers. The main components of the DPT fibres are cellulose 44.17%, hemicellulose 21.95% and lignin 12.75% [23] which was also the case in the current

study but with cellulose and lignin being 34 and 25%, respectively.

2.3. Batch adsorption experiments

All the batch experiments were carried out in triplicate at 30°C in a set of 100 mL conical flasks by shaking at 220 rpm in a temperature-controlled WiseCube® orbital shaker using a fixed mass of 1 g L^{-1} of DPT fibre (particle size 251 μm) and an initial Cu^{2+} metal concentration of 50 mg L^{-1}. Batch experiments to determine equilibration time were conducted over a range of time intervals, from 10 to 180 min., at an initial solution pH of 5.93. pH is one the most important factors governing the process of adsorption [24]. The effect of solution pH on Cu^{2+} adsorption onto DTP was determined in the pH range of 1–6. The effect of various adsorbent doses, i.e. 0.4, 0.6, 0.8, 1, 1.2, 1.4, 1.6, 1.8, 2, 3, 4, and 5 g L^{-1} on the Cu^{2+} removal capacity of DPT biomass was also determined at pH 5. To find the effect of DPT particle size on the removal of Cu^{2+}, different particle sizes were used in the range of 75–251 μm. The effect of metal concentration on the DPT adsorption capacity was also analysed in the range of initial Cu^{2+} 20–100 mg L^{-1}. After shaking, the samples were centrifuged (Elektromag M815P model) at 1,000 rpm for 5 min to separate the adsorbate from the solution and then were filtered using nitrocellulose filter paper (0.45 μm) by vacuum filtration assembly. The residual Cu^{2+} concentration in the filtrate was measured using a flame atomic absorption spectrometer. The amount of adsorbed copper was calculated using Eq. (1):

$$q_e = (C_0 - C_f)V/M \quad (1)$$

where q_e is the metal uptake (mg g^{-1}), and C_0 (mg L^{-1}) and C_f (mg L^{-1}) are the initial and final metal concentration in the solution, respectively. V (L) and M (g) are the solution volume and the mass of the adsorbent, respectively. The sorption percentage (S, %) of the metal ions adsorbed onto DPT fibre biomass was calculated using Eq. (2):

$$S(\%) = \left(\frac{C_0 - C_f}{M}\right)V \times \frac{100}{C_0} \quad (2)$$

2.4. DPT surface characterization

2.4.1. FTIR measurements

DPT fibre adsorbent (75–251 μm), before and after contact with copper aqueous solution, was pelletized using potassium bromide. Then, Fourier transform infrared (FTIR) spectroscopy was carried out to characterize the surface chemistry and the possible functional groups that may participate in adsorption, using the wavenumber region of 500–4,000 cm^{-1}.

2.4.2. XRD measurements

X-ray powder diffraction (XRD) was performed to measure the average crystalline size and surface area of the DPT adsorbent (75–251 μm). Homogeneous alloys were prepared by casting and sintering at 298 K. Afterwards, one gram DPT sample was packed in an aluminium sample holder and analysed with an automated X-ray diffractometer operating at voltage of 40 kV (40 mA current) in the 2θ range from 4° to 30° in steps of 0.02° at a rate of 2.6° per minute using Cu Kα radiations ($\lambda = 1.5418$ nm). The diffractogram showed two sharp peaks at $2\theta = 44.147°$ and 64.5°. The surface area of DPT adsorbent was calculated as 2.104 $m^2\ g^{-1}$, and the average crystalline size of the DPT made from the cellulosic component of the biomass was calculated as 320 nm.

2.4.3. SEM analysis

Scanning electron microscopy (SEM) analysis was performed to study the morphology of the adsorbent material. The samples were mounted on brass stubs using double-sided adhesive tape. SEM photographs were taken with a scanning electron microscope (TESCAN VEGA 3 SBU USA) at various magnifications from ×800 to ×7,500. The working distance of 12.5 mm was maintained, and the images were collected at an acceleration voltage of 5 kV while using a secondary electron detector.

2.5. Isotherms and kinetic models

Equilibrium isotherms were determined by agitating 1 g DPT adsorbent biomass with various concentrations of copper solutions 20–80 mg L^{-1} in a series of 100 mL conical flasks containing 50 mL solution for 180 min at temperature 30°C. Adsorption isotherms are of great importance in designing any adsorption system for the wastewater treatment. Different models including Langmuir, Freundlich, Harkins–Jura (H–J) and Dubinin–Radushkevich (D–R) models were fit to the adsorption kinetic data, and the best fit was determined. The mechanism of Cu^{2+} adsorption onto DPT adsorbent was investigated using pseudo-first-order and pseudo-second-order reaction models.

2.6. Statistical analysis

One-way analysis of variance was carried out to compare the treatment effects on the Cu^{2+} removal capacity of DPT fibre. Different letters on the standard deviation bars indicate significantly different means at $p = 0.01$.

3. Results and discussion

3.1. Effect of contact time on copper adsorption by DPT

Kinetic experiments were conducted in triplicate to find the time taken for the adsorption of Cu^{2+} onto DPT fibre to reach equilibrium (Fig. 1). The data reflected significantly ($p = 0.01$) the higher removal of Cu^{2+} by 90–120 min than in the first 10 min. It was evident that no considerable changes in terms of Cu^{2+} removal were observed after 120 min, and equilibrium was achieved at 150 min.

3.2. Effect of pH on Cu^{2+} removal by DPT

The effect of pH (2–6) on the adsorption of Cu^{2+} onto DPT fibre is shown in Fig. 2(a). Batch experiments were conducted that varied initial Cu^{2+} concentration (50 mg L^{-1}), adsorbent dose (1 g L^{-1}) and temperature (30˚C). The results reflected significantly higher adsorption of Cu^{2+} onto DPT fibre at pH 5 (6 mg g^{-1}, 12%) than at pH 2–4 (1–4 mg g^{-1}, 1–7%) ($p = 0.01$). This higher uptake at less acidic conditions confirms the interference of H^+ ions with metal ions, making it hard for the metal ions to be adsorbed onto the adsorbent surface. Furthermore, the protonation of functional groups on the adsorbent surface leads to the electrostatic repulsion of metal ions, thus minimizing their adsorption [25,26]. The result illustrates that the adsorption of Cu^{2+} onto DPT is not very efficient.

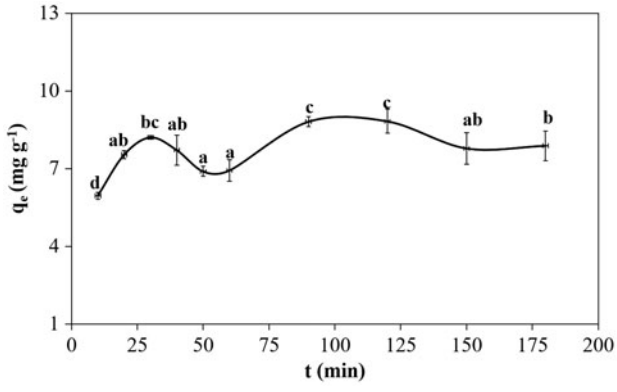

Fig. 1. Effect of contact time on the Cu^{2+} removal capacity (q) of DPT adsorbent.

3.3. Effect of adsorbent dose on Cu^{2+} removal of DPT

The adsorbent dose was varied (0.4–5.0 g L^{-1}), and the rest of experimental variables were held constant (pH 5.0, initial concentration 50 mg L^{-1}, contact time 150 min). The adsorption data revealed significantly ($p = 0.01$) higher removal (25.4 mg g^{-1}) at the adsorbent dose of 5 g L^{-1} compared to the 0.4 g L^{-1} dose at which 3 mg g^{-1} Cu^{2+} removal was observed (Fig. 2(b)). The Cu^{2+} adsorption increased from 6 to 51% with an increase in the adsorbent dose from 0.4 to 5.0 g L^{-1}. The reasons for this increase could be the larger surface area and more available binding sites or more functional groups resulting from the increased amount of adsorbent [16,18].

3.4. Effect of particle size on Cu^{2+} removal of DPT

The effect of particle size on the amount of Cu^{2+} removed is shown in Fig. 3(a). Significantly higher removal (34 mg g^{-1}) was observed with particles 75 μm large compared to larger particle size (251 μm). However, Cu^{2+} removal was only 14% higher (68%, 75 μm of particle size) compared to 54% Cu^{2+} removal at larger particle size (100–251 μm). Smaller particles offer more surface area to the metal ions present in the aqueous solution [27].

3.5. Effect of initial Cu^{2+} concentration

The effect of initial Cu^{2+} concentration on its removal by DPT is shown in Fig. 3(b). Cu^{2+} removal was significantly higher (6–23 mg g^{-1}) with increasing Cu^{2+} concentration from 20 to 100 mg L^{-1}. The driving force of concentration gradient inherent to an increase in the initial concentrations of Cu^{2+} may overcome the resistance to mass transfer at the adsorbent surface. However, the per cent removal of Cu^{2+} decreased from 31 to 23% at higher Cu^{2+} concentrations, probably due to the saturation of sorption sites at the adsorbent surface [19,28].

3.6. Adsorption isotherms

Adsorption isotherms are of fundamental importance in the design of adsorption systems. The Cu^{2+} adsorption data were further analysed using the most frequently applied models, i.e. Langmuir and Freundlich's models [29]. The experimental data were fitted to these isotherms to describe the solutes' adsorption [27].

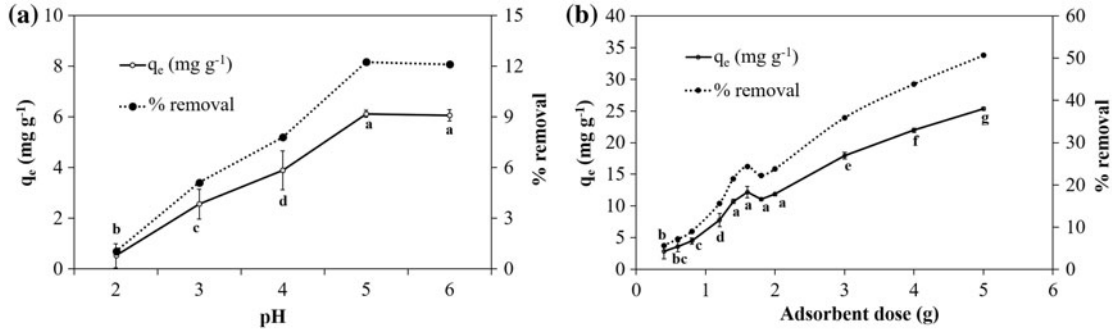

Fig. 2. Effect of pH (a) and adsorbent dose (b) on the Cu^{2+} removal capacity (q_e) of DPT fibre.

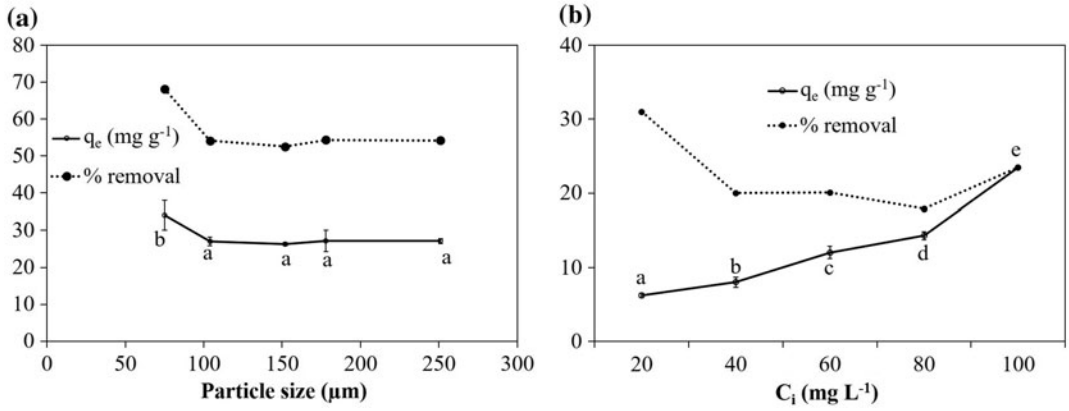

Fig. 3. Effect of particle size (a) and initial concentration of Cu^{2+} (b) on the Cu^{2+} removal capacity (q_e) of DPT fibre.

3.6.1. Langmuir isotherm model

This model assumes (i) monolayer coverage; (ii) that all active adsorption sites are equally probable with the same energy. The Langmuir model can be written using Eq. (3):

$$q_e = (q_{max} K_{ads} C_e)/1 + K_{ads} C_e \quad (3)$$

where q_e (mg g^{-1}) is the amount of Cu^{2+} adsorbed at equilibrium, q_{max} is the maximal metal concentration attained in monolayer coverage, C_e is the metal ion concentration in solution and K_{ads} (L mg^{-1}) is the Langmuir adsorption constant, which is related to the free energy of adsorption and applied temperature.

Eq. (3) can be linearized into Langmuir isotherm form, as written in the form of Eq. (4):

$$\frac{1}{q_e} = \frac{1}{q_{max}} + \left(\frac{1}{q_{max} K_{ads}}\right)\frac{1}{C_e} \quad (4)$$

The fit of the equilibrium data to Langmuir isotherms was evaluated using plots of $1/q_e \sim 1/C_e$.

q_{max} and K_{ads} can be calculated from intercept and slope of the plot of $1/q_e \sim 1/C_e$, i.e. q_{max} = 1/intercept and K_{ads} = intercept/slope, for $1/q_{max}$ and $1/(K_{ads}q_{max})$ are the slope and intercept, respectively (Eq. (4)). In this study, a Langmuir isotherm model was used to describe the relationship between adsorbed Cu^{2+} and its equilibrium concentration at 30°C, pH 5, adsorbent dose of 1 g L^{-1} for 50 mg L^{-1} initial Cu^{2+} concentration and duration of 3 h. The predicted maximum adsorption capacity (q_{max}) was slightly higher (25 mg g^{-1}) than the experimentally attained value (q_e = 23.5 mg g^{-1}), indicative of saturation of DPT adsorbent capacity at higher initial Cu^{2+} concentration (Table 1).

The linearized plot of Langmuir isotherm had the best fit to experimental data, with an R^2 value of 0.9933 (Fig. 4(a)). A regression coefficient (R^2) closer to unity expresses a better fit of the isotherm equation to the adsorption data, while one approaching zero represents the opposite case [30]. The linear plot

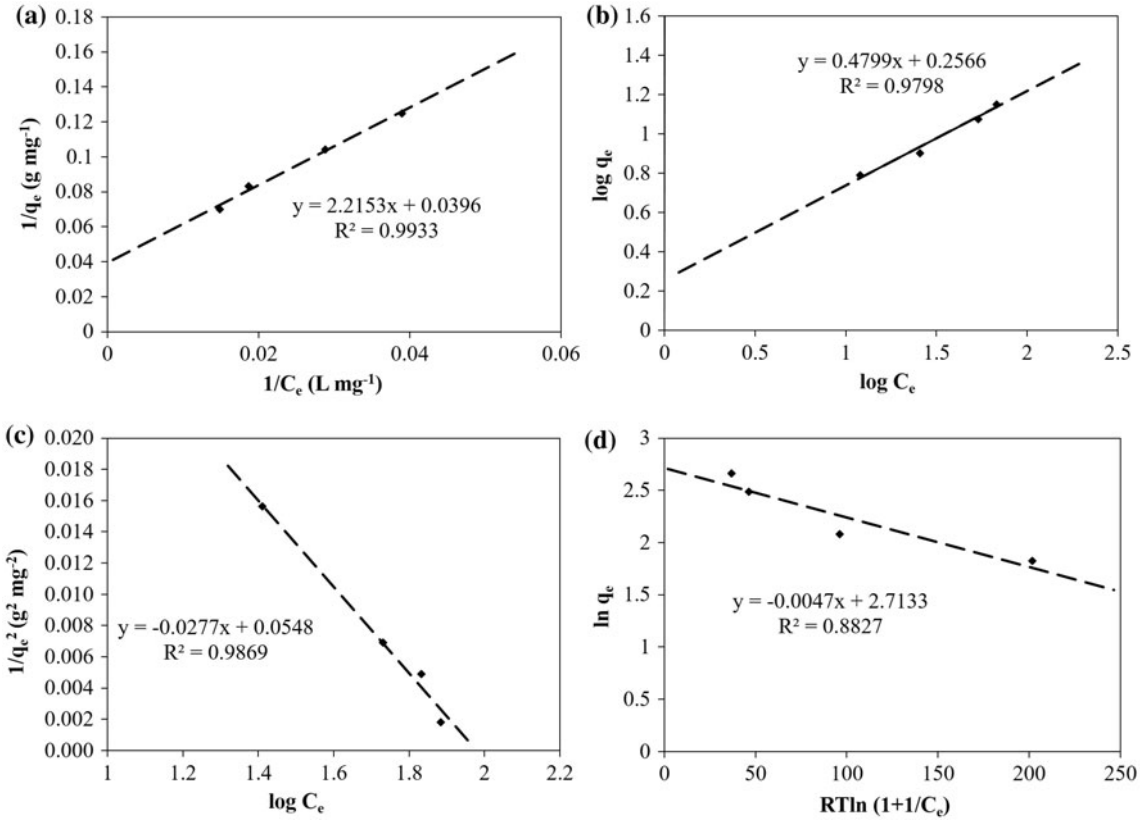

Fig. 4. Adsorption of Cu^{2+} onto DPT fibre: (a) Langmuir isotherm, (b) Freundlich isotherm, (c) Harkins–Jura isotherm, and (d) Dubinin–Radushkevich isotherm.

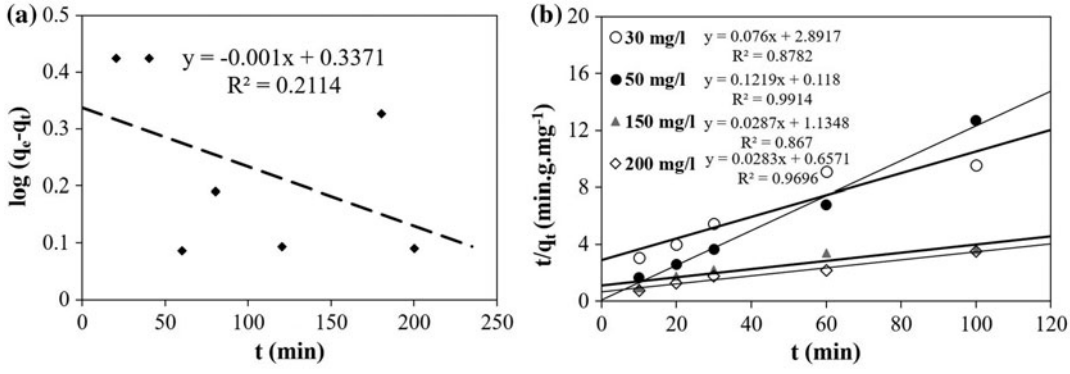

Fig. 5. Pseudo-second-order kinetic plot of Cu^{2+} adsorption onto DPT fibre.

($R^2 = 0.9967$) of $1/q_e \sim 1/C_e$ at 30°C indicates the applicability of Langmuir isotherm to the adsorption process. The Langmuir adsorption isotherm assumes the monolayer coverage of the adsorbate onto the active sites on the surface of adsorbent [31]. The good fit of the Langmuir isotherm indicates that the adsorption of Cu^{2+} onto the investigated sorbent (DPT adsorbent) forms a monolayer, and the surface of adsorbent seems uniform. Moreover, the formation of a monolayer of Cu^{2+} ions on the surface of DPT adsorbent hinders the formation of any further metal layer because of the interaction between metal ions on the surface of the DPT adsorbent and in the bulk of solution [32].

The separation factor or equilibrium parameter R can also be used to describe the essential

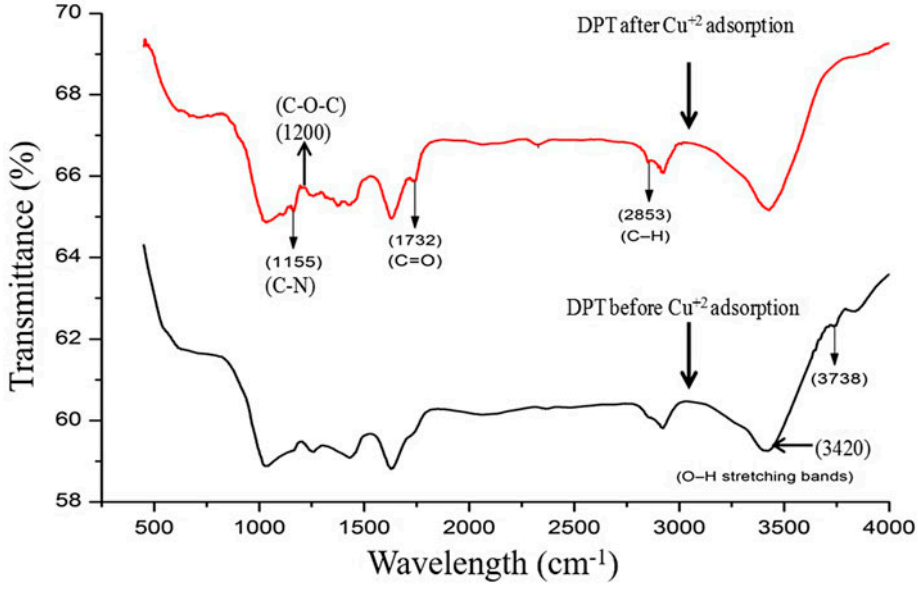

Fig. 6. FTIR spectra of DPT before and after Cu^{2+} adsorption in the 500–4,000 cm^{-1} wave number region.

characteristics of the Langmuir isotherms through a dimensionless constant [33], which is defined by Eq. (5):

$$R = \frac{1}{1 + bC_0} \tag{5}$$

where b is the Langmuir constant and C_0 is the initial concentration of Cu^{2+}, 50 mg L^{-1}. The isotherm shape (R) can be used to predict whether adsorption is favourable or unfavourable. Adsorption of any pollutant is regarded favourable if $0 < R_L < 1$, unfavourable if $R_L > 1$, linear if $R_L = 1$ and irreversible if $R_L = 0$. In the current study, $R = 0.3576 < 1$, which reflects the favourable adsorption and strong binding between Cu^{2+} and DPT adsorbent in the present system. This means that DPT adsorbent requires fewer operation steps to obtain high removal of Cu^{2+} and, therefore, DPT can be used efficiently at large scale. DPT fibre displayed a maximum adsorption (q_{max}) capacity of Cu^{2+} of 25 mg g^{-1}, which is higher than the q_{max} of wheat shell (17.42 mg g^{-1}), spent grains (10.47 mg g^{-1}), tea industry waste (8.64 mg g^{-1}), tobacco fibre (10.5 mg g^{-1}), rice husk (31.85 mg g^{-1}) and cotton boll (11.40 mg g^{-1}) (Table 2).

3.6.2. Freundlich isotherm model

This model is an exponential relationship (Eqs. (6a) and (6b)); it assumes that the adsorbate concentration on the adsorbent surface increases when the adsorbate concentration increases in the solution [42]. This model is used to describe the adsorption of a heterogeneous system with multilayer adsorption, and the adsorption capacity is dependent on the concentration of adsorbate at equilibrium:

$$q_e = K_F C_e^{\frac{1}{n}} \tag{6a}$$

$$\log q_e = \log K_F + \frac{1}{n}\log C_e \quad \text{(Linear form)} \tag{6b}$$

where K_F is the Freundlich constant (mg g^{-1}) and $1/n$ is the adsorption intensity. Both K_F and $1/n$ can be calculated from the slope and intercept in the linear plot of log q_e vs log C_e. The magnitude of the exponent n shows the favourability of adsorption. $1/n$ values can indicate the isotherm to be favourable ($0 < 1/n < 1$), irreversible ($1/n = 0$) or unfavourable ($1/n > 1$) [43]. The higher the fractional value, the higher the heterogeneity of the adsorbent surface [44]. This study showed $0.4818 = 1/n$, which reflected favourable adsorption under studied conditions. Using $n = 2.07$, the value of K_F is 1.43 L g^{-1}, which is higher than that of cedar sawdust, i.e. 0.59, $n = 1.02$ [45].

The maximum adsorption capacity was determined by operating with constant initial concentration C_0 and variable adsorbent doses (Eq. (7)); thus, log q_m is the extrapolated value of log q when $C = C_0$.

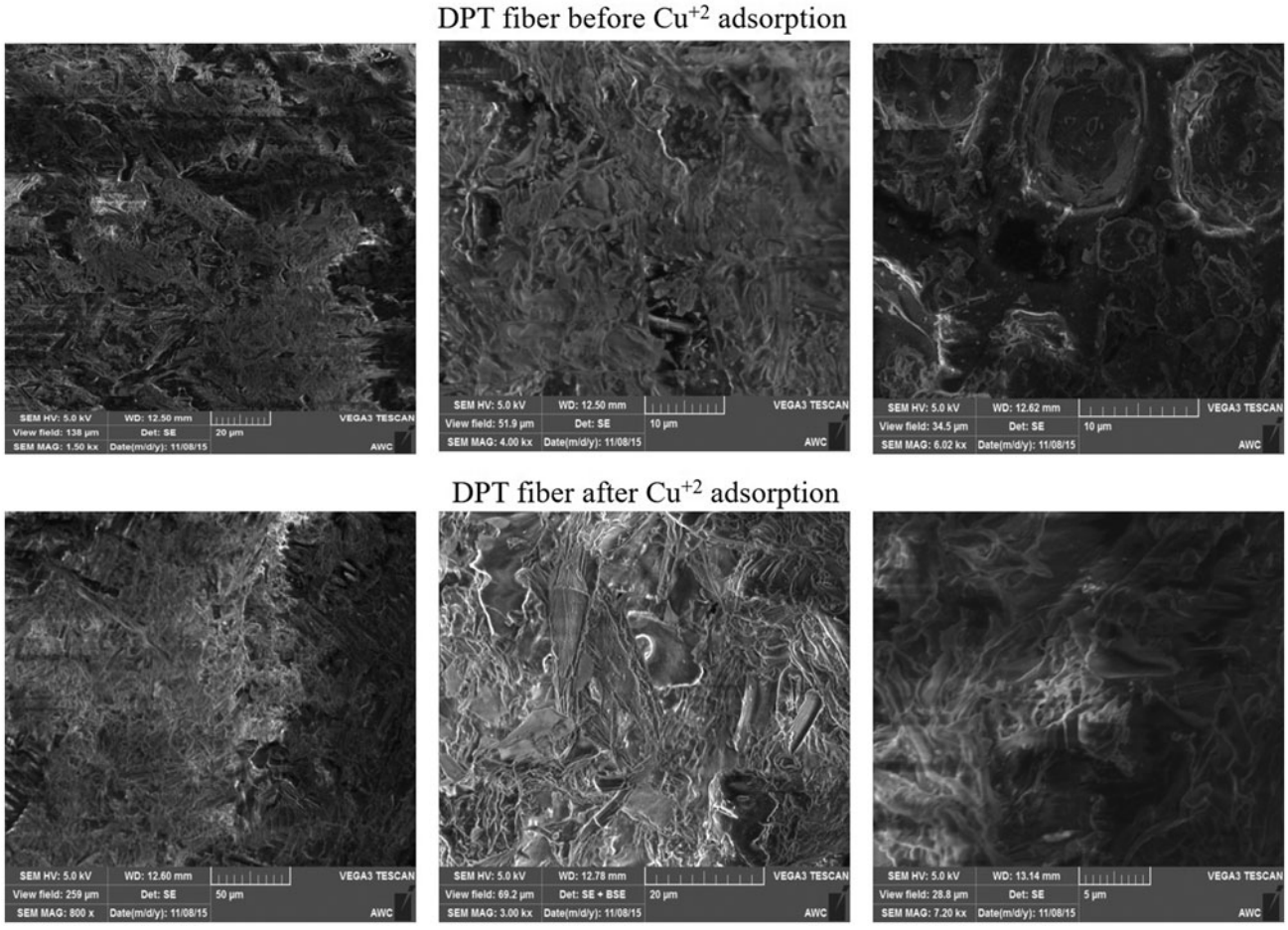

Fig. 7. SEM photographs of DPT fibre before and after Cu^{2+} adsorption at different magnifications.

$$K_F = \frac{q_m}{C_0^{\frac{1}{n}}} \quad (7)$$

where C_0 is the initial concentration of Cu^{2+} in the bulk solution (mg L^{-1}) and q_m is the Freundlich maximum adsorption capacity (mg g^{-1}). In the current study, the Freundlich maximum absorption capacity (q_m) of DPT for Cu^{2+} was 10.73 mg g^{-1} (Table 1), which was lower than the q_{max} calculated from the Langmuir isotherm (23 mg g^{-1}). The R^2 value from the Langmuir isotherm (0.9933) was higher than that of the Freundlich isotherm (0.9798) (Fig. 4(b)) which reflects monolayer adsorption in the system.

3.6.3. Harkins–Jura isotherm

This isotherm assumes multilayer adsorption with the existence of heterogeneous pore diffusion. It can be expressed using Eq. (8):

$$\frac{1}{q_e^2} = \frac{B}{A} - \left(\frac{1}{A}\right) \log C_e \quad (8)$$

where B and A are H–J's constants (Table 1). The H–J isotherm parameters are obtained from the slope and intercept of the plots of $1/q_e^2$ vs. log C_e. The H–J isotherm fits the experimental data better (R^2 = 0.9869) than the Freundlich and D–R isotherms, but worse than the Langmuir, which does not model any multilayer adsorption of Cu^{2+} ions on the DPT adsorbent, as indicated by the R^2 values in Table 1 and Fig. 4(c).

3.6.4. Dubinin–Radushkevich isotherm

The type of sorption (physical or chemical) was determined by fitting the equilibrium data to the D–R isotherm model [46,47]. The linear form of D–R isotherm can be written using Eq. (9):

Table 1
Constants for different isotherm models at 50 mg L^{-1} initial Cu^{2+} concentration at 30°C

Parameter	Value
Experimental	
q_e (mg g^{-1})	23.4
Langmuir isotherms	
q_{max} (mg g^{-1})	25.25
K_{ads} (L mg^{-1})	0.018
R^2	0.9934
H–J	
A	36.1011
B	1.978339
R^2	0.9869
Freundlich isotherm	
$1/n$	0.4818
n	2.0757
K_F (L g^{-1})	1.43
q_m (mg g^{-1})	10.72
R^2	0.9798
D–R	
q_{DR} (mol g^{-1})	15.08
β (mol $J^{-1})^2$	0.0047
E (kJ mol^{-1})	14.5865
R^2	0.8827

Table 2
Maximum of Cu^{2+} adsorption capacity (q_{max}) of different low-cost and easily available biosorbents

Adsorbent	Cu^{2+} uptake (mg g^{-1})	Refs.
Wheat shells	17.42	[34]
Spent grain	10.47	[35]
Tea industry waste	8.64	[36]
Tobacco fibre	10.5	[37]
Rice husk	31.85	[38]
Banana peels	4.75	[39]
Orange peels	3.65	[40]
Cotton boll	11.40	[40]
Corn cobs	7.62	[41]
Date palm trunk fibre	25.25	Current study

$$\ln q_e = \ln q_{DR} - \beta\varepsilon^2 \quad (9)$$

where q_e is the amount of Cu^{2+} adsorbed per unit weight of DPT adsorbent (mol g^{-1}), q_{DR} is the theoretical monolayer sorption capacity (mol g^{-1}), β is the constant sorption energy ($mol^2\ J^{-2}$), which is related to the average energy of sorption per mole of adsorbate when it is transferred to the solid surface from an infinite distance in the solution. is the Polanyi potential, which can be obtained by Eq. (10), where T is the solution temperature (K) and R is the gas constant (8.314 J $mol^{-1}\ K^{-1}$).

$$\varepsilon = RT \ln\left[1 + \frac{1}{C_e}\right] \quad (10)$$

where the average energy of adsorption (E) can be determined using Eq. (11).

$$E = \frac{1}{\sqrt{-2\beta}} \quad (11)$$

The value of E reflects the physical and chemical nature of adsorption (Eq. (11)). It ranges from 1 to 8 kJ mol^{-1} for physical and 8 to 16 kJ mol^{-1} for chemical sorption. The E value for DPT adsorbent was found to be 14.59 kJ mol^{-1} which revealed the chemisorptive nature of Cu^{2+} adsorption [48]. However, D–R model showed a worse fit to the experimental data ($R^2 = 0.8827$, Fig. 4(d)) than Langmuir, H–J and Freundlich isotherms models under the studied conditions.

3.7. Kinetic modelling

Various kinetic models, i.e. pseudo-first order and pseudo-second order were used to study the transient behaviour of the batch adsorption at 50 mg L^{-1} Cu^{2+} concentration.

3.7.1. Pseudo-first-order kinetic model

Solid adsorbent capacity can be described by a pseudo-first-order rate model [49], expressed in the linearized form using Eq. (12):

$$\log(q_e - q_t) = \log q_e - k_1 t/2.303 \quad (12)$$

where q_e is the amount of Cu^{2+} adsorbed at equilibrium per unit mass of adsorbent (mg g^{-1}), q_t is the amount of Cu^{2+} adsorbed at time t (mg g^{-1}) and k_1 (h^{-1}) is the adsorption rate constant for the pseudo-first-order rate model.

The coefficient of determination (R^2) of the linear regression of the plot ($\log(q_e - q_t) \sim t$)) in Eq. (12) was low, as shown in Fig. 5(a). Therefore, the adsorption kinetics of Cu^{2+} on DPT are poorly described by a pseudo-first-order model.

Table 3
Pseudo-second-order models for Cu^{2+} adsorption on DPT

Initial Cu^{2+} concentration (mg L^{-1})	q_e experiment (mg g^{-1})	K_2 (g mg^{-1} min^{-1})	q cal (mg g^{-1})	R^2
30	20.95	0.002	13.16	0.8782
50	8.83	0.123	8.20	0.9914
150	54.63	0.001	34.84	0.867
200	56.8	0.001	35.34	0.9696

3.7.2. Pseudo-second-order kinetic model

The linearized form of pseudo-second-order model [50] has been used by Yadav and co-researchers [51] for divalent metal adsorption onto adsorbents. This model is based on solid-phase sorption, which can be written using the Eq. (13):

$$\frac{t}{q_t} = \frac{1}{k_2 q_e^2} + \frac{1}{q_e} t \tag{13}$$

where q_e is the total Cu^{2+} adsorption capacity, q_t is the amount of Cu^{2+} adsorbed at time t (min) and k_2 is the pseudo-second-order rate constant (g mg^{-1} min^{-1}). A plot of (t/q_t ~ t) displayed a linear relationship at 50 mg L^{-1} of initial ion concentration (Fig. 5(b)).

The values of k_2 (g mg^{-1} min^{-1}) and q_e (mg g^{-1}) were calculated from the slope and intercept of the plot t/q_t ~ t. It was observed from the plot (t/q_t ~ t) (Eq. (12)) that the coefficient of determination R^2 is 0.9905, which is very close to unity, and $q_{e(cal)}$ agreed with the experimental adsorption capacity (Table 3) at 50 mg L^{-1} initial dye concentration.

Poor correlations were observed at 30, 150, and 200 mg L^{-1} initial concentrations of Cu^{2+}. Therefore, q_{cal} values predicted by the model were also not in agreement with the experimental adsorption capacity. This also reflects that pseudo-second-order model is more likely to describe the kinetic behaviour of Cu^{2+} adsorption onto DPT fibre at lower concentrations of the adsorbate. The good fit of the pseudo-second-order model supports the assumption underlying that model of the chemisorption being the rate-controlling step.

3.8. DPT surface characterization

3.8.1. FTIR analysis

Fig. 6 reflects the various functional groups present on the surface of DPT fibre biomass. The absorption peaks at 3,400 cm^{-1} are assigned to O–H stretching on the surface of DPT biomass. Similarly, the absorptive peak at 2,853, 1,732, and 1,155 cm^{-1} represents the functional groups of hydrocarbon (C–H), carbonyl (C=O) and C–N, respectively, which may participate in and enhance Cu^{2+} ion adsorption. The functional group (C=O) at 1,736 cm^{-1} has also been observed in the date palm pits by Al-Saidi [52] to be involved in gold adsorption. Peaks recorded in the range 1,600 cm^{-1} confirm the presence of C–C bonding, peculiar to aromatic compounds.

A sharp peak noticed at 2,853 cm^{-1} demonstrates the existence of aldehyde groups at the adsorbent surface. At equilibrium adsorption, the disappearance of two peaks at 1,732 and 3,738 cm^{-1} confirms the involvement of unsaturated esters and hydroxyl groups from $Si^{18}OH$ in the adsorption of copper from the aqueous solution [53]. The availability of hydroxyl groups on the surface of adsorbent has enhanced the process of chemisorption through formation of Cu^{2+} hydroxide complexes. Shifting of vibration frequencies (band intensities for the whole spectra) validates the formation of new bonds between the functional groups on the adsorbent surface and adsorbate in solution [54]. Similar shifts in band intensity have been reported for FTIR spectra of sugarcane bagasse before and after dye removal [55].

3.8.2. SEM analyses

SEM analysis was carried out to obtain insight into how the surfaces of DPT fibres look before and after Cu^{2+} adsorption onto the surface of DPT (Fig. 7). SEM photographs showed asymmetric pores that were rough and cylinders on the surface of the DPT fibres before Cu^{2+} adsorption.

These cylinders seem to be composed of multicellular fibres bound together by lignin. The rough surface of the DPT fibre can improve the interaction with the Cu^{2+} metal ions. One can also observe the central void inside the fibre, known as the lumen. After Cu^{2+} adsorption, the surface of a DPT fibre takes on a rather smooth and shiny appearance with closed pore structures, which can be attributed to physicochemical interaction between the contaminant and the functional groups present on the surface of the DPT fibre. The change of the structure of DPT fibre surface can be linked to the influence of metal ions.

4. Conclusions

The search for low-cost adsorbents that are readily available in bulk, with high capacities for toxic metal ion uptake, is an active area of research worldwide. The experimental data reflected the significantly higher removal of Cu^{2+} by 90–120 min, and the equilibrium was achieved at 150 min. The effect of pH (2–6) on the adsorption of Cu^{2+} onto DPT fibre revealed significantly higher adsorption of Cu onto DPT fibre at pH 5 (6 mg g^{-1}, 12%) than at pH 2–4 (1–4 mg g^{-1}, 1–7%) ($p = 0.01$). For the effects of adsorbent dose and particle size, the adsorption data revealed significantly high removal (25.4 mg g^{-1}) at the adsorbent dose of 5 g L^{-1} and particles size of 75 μm. Cu^{2+} removal was significantly higher (6–23 mg g^{-1}) with increasing Cu^{2+} concentration from 20 to 100 mg L^{-1}; however, it decreased from 31 to 23% at higher Cu^{2+} concentrations.

The behaviour and the nature of Cu^{2+} adsorption were analysed by employing different isotherm models, and the results fitted the experimental data in the following order: Langmuir > H–J > Freundlich > D–R with monolayer Cu^{2+} adsorption. Also, the adsorption kinetics data were modelled using pseudo-first-order and pseudo-second-order kinetics, and the experimental data were best explained by pseudo-second-order kinetics ($R^2 = 0.9905$) and q_{max} of 25.25 mg g^{-1} with chemisorption ($E = 14.59$ kJ mol^{-1}). The present investigation of waste DPT fibre for the removal of Cu^{2+} emphatically showed the possibility of using it as an adsorbing material. There is still room for further investigation because of the complex and diverse chemical composition of real wastewaters that contain a variety of toxic metals and that change over time. However, the cost of the adsorbent is also an important economic issue from economical aspect, which must be considered when selecting an adsorbent.

Acknowledgements

"This project was funded by the National Plan for Science, Technology and Innovation (MAARIFAH), King Abdulaziz City for Science and Technology, Kingdom of Saudi Arabia, Award Number (11-WAT1875-02)".

References

[1] M. Bilal, J.A. Shah, T. Ashfaq, S.M.H. Gardazi, A.A. Tahir, A. Pervez, H. Haroon, Q. Mahmood, Waste biomass adsorbents for copper removal from industrial wastewater—A review, J. Hazard. Mater. 263 (2013) 322–333.

[2] V.J. Inglezakis, M.D. Loizidou, H.P. Grigoropoulou, Ion exchange of Pb^{2+}, Cu^{2+}, Fe^{3+}, and Cr^{3+} on natural clinoptilolite: Selectivity determination and influence of acidity on metal uptake, J. Colloid Interface Sci. 261 (2003) 49–54.

[3] M.H. Kalavathy, T. Karthikeyan, S. Rajgopal, L.R. Miranda, Kinetic and isotherm studies of Cu(II) adsorption onto H_3PO_4-activated rubber wood sawdust, J. Colloid Interface Sci. 292 (2005) 354–362.

[4] J.P. Chen, J.T. Yoon, S. Yiacoumi, Effects of chemical and physical properties of influent on copper sorption onto activated carbon fixed-bed columns, Carbon 41 (2003) 1635–1644.

[5] A. Kapoor, T. Viraraghavan, Removal of heavy metals from aqueous solutions using immobilized fungal biomass in continuous mode, Water Res. 32 (1998) 1968–1977.

[6] M. Varga, M. Takács, G. Záray, I. Varga, Comparative study of sorption kinetics and equilibrium of chromium (VI) on charcoals prepared from different low-cost materials, Microchem. J. 107 (2013) 25–30.

[7] V.K. Gupta, A. Rastogi, V.K. Saini, N. Jain, Biosorption of copper(II) from aqueous solutions by *Spirogyra* species, J. Colloid Interface Sci. 296 (2006) 59–63.

[8] G. Popescu, L. Dumitru, Biosorption of Some heavy metals from media with high salt concentrations by halophilic *Archaea*, Biotechnol. Biotechnol. Equip. 23 (2009) 791–795.

[9] M.Y. Pamukoglu, F. Kargi, Removal of copper(II) ions from aqueous medium by biosorption onto powdered waste sludge, Process Biochem. 41 (2006) 1047–1054.

[10] V.K. Gupta, A. Rastogi, Biosorption of lead from aqueous solutions by green algae *Spirogyra* species: Kinetics and equilibrium studies, J. Hazard. Mater. 152 (2008) 407–414.

[11] A. Rathinam, B. Maharshi, S.K. Janardhanan, R.R. Jonnalagadda, B.U. Nair, Biosorption of cadmium metal ion from simulated wastewaters using Hypnea valentiae biomass: A kinetic and thermodynamic study, Bioresour. Technol. 101 (2010) 1466–1470.

[12] M. Auta, B.H. Hameed, Coalesced chitosan activated carbon composite for batch and fixed-bed adsorption of cationic and anionic dyes, Colloids Surf., B: Biointerfaces 105 (2013) 199–206.

[13] J. Galán, A. Rodríguez, J.M. Gómez, S.J. Allen, G.M. Walker, Reactive dye adsorption onto a novel mesoporous carbon, Chem. Eng. J. 219 (2013) 62–68.

[14] B. Ismail, S.T. Hussain, S. Akram, Adsorption of methylene blue onto spinel magnesium aluminate nanoparticles: Adsorption isotherms, kinetic and thermodynamic studies, Chem. Eng. J. 219 (2013) 395–402.

[15] R. Ansari, Z. Mosayebzadeh, Removal of basic dye methylene blue from aqueous solutions using sawdust and sawdust coated with polypyrrole, J. Iran. Chem. Soc. 7 (2010) 339–350.

[16] D. Uzunoğlu, N. Gürel, N. Özkaya, A. Özer, The single batch biosorption of copper(İI) ions on *Sargassum acinarum*, Desalin. Water Treat. 52 (2014) 1514–1523.

[17] A.A. Bsoul, L. Zeatoun, A. Abdelhay, M. Chiha, Adsorption of copper ions from water by different types of natural seed materials, Desalin. Water Treat. 52 (2014) 5876–5882.

[18] H. Aydın, Y. Bulut, Ç. Yerlikaya, Removal of copper (II) from aqueous solution by adsorption onto low-cost adsorbents, J. Environ. Manage. 87 (2008) 37–45.
[19] W.P. Putra, A. Kamari, S.N.M. Yusoff, C.F. Ishak, A. Mohamed, N. Hashim, I.M. Isa, Biosorption of Cu(II), Pb(II) and Zn(II) ions from aqueous solutions using selected waste materials: Adsorption and characterisation studies, J. Encapsulation Adsorpt. Sci. 04 (2014) 25–35.
[20] T.-C. Hsu, Experimental assessment of adsorption of Cu^{2+} and Ni^{2+} from aqueous solution by oyster shell powder, J. Hazard. Mater. 171 (2009) 995–1000.
[21] X. Guo, S. Zhang, X. Shan, Adsorption of metal ions on lignin, J. Hazard. Mater. 151 (2008) 134–142.
[22] N. Ertugay, Y.K. Bayhan, The removal of copper (II) ion by using mushroom biomass (*Agaricus bisporus*) and kinetic modelling, Desalination 255 (2010) 137–142.
[23] J.S. Macedo, L. Otubo, O.P. Ferreira, I.d.F. Gimenez, I.O. Mazali, L.S. Barreto, Biomorphic activated porous carbons with complex microstructures from lignocellulosic residues, Microporous Mesoporous Mater. 107 (2008) 276–285.
[24] M.M. Areco, M. Dos Santos Afonso, Copper, zinc, cadmium and lead biosorption by *Gymnogongrus torulosus* thermodynamics and kinetics studies, Colloids Surf., B: Biointerfaces 81 (2010) 620–628.
[25] H.I. Chieng, L.B.L. Lim, N. Priyantha, Enhancing adsorption capacity of toxic malachite green dye through chemically modified breadnut peel: Equilibrium, thermodynamics, kinetics and regeneration studies, Environ. Technol. 36 (2015) 86–97.
[26] A.A. El-Bindary, M.A. Hussien, M.A. Diab, A.M. Eessa, Adsorption of Acid Yellow 99 by polyacrylonitrile/activated carbon composite: Kinetics, thermodynamics and isotherm studies, J. Mol. Liq. 197 (2014) 236–242.
[27] M.A. Al-Ghouti, J. Li, Y. Salamh, N. Al-Laqtah, G. Walker, M.N.M. Ahmad, Adsorption mechanisms of removing heavy metals and dyes from aqueous solution using date pits solid adsorbent, J. Hazard. Mater. 176 (2010) 510–520.
[28] A.A. Al-Homaidan, H.J. Al-Houri, A.A. Al-Hazzani, G. Elgaaly, N.M.S. Moubayed, Biosorption of copper ions from aqueous solutions by *Spirulina platensis* biomass, Arab. J. Chem. 7 (2014) 57–62.
[29] L.D. Benefield, J.F. Judkins, B.L. Weand, Process chemistry for water and wastewater treatment, Prentice-Hall, Ontario, Canada, 1982.
[30] M.S. Rahman, M.R. Islam, Effects of pH on isotherms modeling for Cu(II) ions adsorption using maple wood sawdust, Chem. Eng. J. 149 (2009) 273–280.
[31] M. Nadeem, A. Mahmood, S.A. Shahid, S.S. Shah, A.M. Khalid, G. McKay, Sorption of lead from aqueous solution by chemically modified carbon adsorbents, J. Hazard. Mater. 138 (2006) 604–613.
[32] T.W. Weber, R.K. Chakravorti, Pore and solid diffusion models for fixed-bed adsorbers, AIChE J. 20 (1974) 228–238.
[33] K.R. Hall, L.C. Eagleton, A. Acrivos, T. Vermeulen, Pore- and solid-diffusion kinetics in fixed-bed adsorption under constant-pattern conditions, Ind. Eng. Chem. Fundam. 5 (1966) 212–223.
[34] H. Aydın, Y. Bulut, Ç. Yerlikaya, Removal of copper (II) from aqueous solution by adsorption onto low-cost adsorbents, J. Environ. Manage. 87 (2008) 37–45.
[35] S. Lu, S.W. Gibb, Copper removal from wastewater using spent-grain as biosorbent, Bioresour. Technol. 99 (2008) 1509–1517.
[36] S. Çay, A. Uyanık, A. Özaşık, Single and binary component adsorption of copper(II) and cadmium(II) from aqueous solutions using tea-industry waste, Sep. Purif. Technol. 38 (2004) 273–280.
[37] A. Demirbas, Heavy metal adsorption onto agro-based waste materials: A review, J. Hazard. Mater. 157 (2008) 220–229.
[38] K.K. Wong, C.K. Lee, K.S. Low, M.J. Haron, Removal of Cu and Pb from electroplating wastewater using tartaric acid modified rice husk, Process Biochem. 39 (2003) 437–445.
[39] M. Ajmal, R.A.K. Rao, R. Ahmad, J. Ahmad, Adsorption studies on Citrus reticulata (fruit peel of orange): Removal and recovery of Ni(II) from electroplating wastewater, J. Hazard. Mater. 79 (2000) 117–131.
[40] H.D. Ozsoy, H. Kumbur, Adsorption of Cu(II) ions on cotton boll, J. Hazard. Mater. 136 (2006) 911–916.
[41] Z. Reddad, C. Gerente, Y. Andres, P. Le Cloirec, Adsorption of several metal ions onto a low-cost biosorbent: Kinetic and equilibrium studies, Environ. Sci. Technol. 36 (2002) 2067–2073.
[42] H.M.F. Freundlich, Over the adsorption in solution, J. Phys. Chem. 57 (1906) 385–470.
[43] C. Ng, J.N. Losso, W.E. Marshall, R.M. Rao, Freundlich adsorption isotherms of agricultural by-product-based powdered activated carbons in a geosmin–water system, Bioresour. Technol. 85 (2002) 131–135.
[44] R. Djeribi, O. Hamdaoui, Sorption of copper(II) from aqueous solutions by cedar sawdust and crushed brick, Desalination 225 (2008) 95–112.
[45] R. Djeribi, O. Hamdaoui, Sorption of copper(II) from aqueous solutions by cedar sawdust and crushed brick, Desalination 225 (2008) 95–112.
[46] M.M. Dubinin, The potential theory of adsorption of gases and vapors for adsorbents with energetically nonuniform surfaces, Chem. Rev. 60 (1960) 235–241.
[47] N.D. Hutson, R.T. Yang, Theoretical basis for the Dubinin-Radushkevitch (D-R) adsorption isotherm equation, Adsorption 3 (1997) 189–195.
[48] A. Sarı, M. Tuzen, D. Cıtak, M. Soylak, Adsorption characteristics of Cu(II) and Pb(II) onto expanded perlite from aqueous solution, J. Hazard. Mater. 148 (2007) 387–394.
[49] S. Lagergren, About the theory of so-called adsorption of soluble substances, K. Sven. Vetenskapsakademiens Handl. 24 (1898).
[50] S. Liang, X. Guo, N. Feng, Q. Tian, Application of orange peel xanthate for the adsorption of Pb^{2+} from aqueous solutions, J. Hazard. Mater. 170 (2009) 425–429.
[51] S.K. Yadav, D.K. Singh, S. Sinha, Adsorption study of lead(II) onto xanthated date palm trunk: Kinetics, isotherm and mechanism, Desalin. Water Treat. 51 (2013) 6798–6807.

[52] H.M. Al-Saidi, The fast recovery of gold(III) ions from aqueous solutions using raw date pits: Kinetic, thermodynamic and equilibrium studies, J. Saudi Chem. Soc. (in press), doi: 10.1016/j.jscs.2013.06.002.
[53] E.F. Vansant, P.V.D. Voort, K.C. Vrancken, Characterization and Chemical Modification of the Silica Surface, Elsevier, Amsterdam, 1995.
[54] G. Gebrehawaria, A. Hussen, V.M. Rao, Removal of hexavalent chromium from aqueous solutions using barks of *Acacia albida* and leaves of *Euclea schimperi*, Int. J. Environ. Sci. Technol. 12 (2015) 1569–1580.
[55] Z. Zhang, I.M. O'Hara, G.A. Kent, W.O.S. Doherty, Comparative study on adsorption of two cationic dyes by milled sugarcane bagasse, Ind. Crops Prod. 42 (2013) 41–49.